We are IntechOpen, the world's leading publisher of Open Access books Built by scientists, for scientists

5,300
Open access books available

130,000
International authors and editors

155M
Downloads

Our authors are among the

154
Countries delivered to

TOP 1%
most cited scientists

12.2%
Contributors from top 500 universities

CLARIVATE ANALYTICS BOOK CITATION INDEX INDEXED

WEB OF SCIENCE™

Selection of our books indexed in the Book Citation Index in Web of Science™ Core Collection (BKCI)

Interested in publishing with us?
Contact book.department@intechopen.com

Numbers displayed above are based on latest data collected.
For more information visit www.intechopen.com

7

π-SIFT: A Photometric and Scale Invariant Feature Transform

Jae-Han Park, Kyung-Wook Park,
Seung-Ho Baeg and Moon-Hong Baeg
Korea Institute of Industrial Technology (KITECH)
South Korea

1. Introduction

For many years, various local descriptors that are insensitive to geometric changes such as viewpoint, rotation, and scale changes, have been attracting attention due to their promising performance. However, most existing local descriptors including the SIFT are based on luminance information rather than colour information thereby resulting in instability to photometric variations such as shadows, highlights, and illumination changes. In this paper, we propose a novel local descriptor, PI-SIFT, that are invariant to both geometric and photometric variations. In order to achieve photometric invariance, we adopt photometric quasi-invariant features based on the dichromatic reflection model and for geometric invariance, the Scale Invariant Feature Transform (SIFT) is used. The performance of the proposed descriptor is evaluated with other local descriptors. Experimental results show that our descriptor gives similar performance or outperforms them with respect to imaging conditions including photometric and geometric variations.

In computer vision, the need for a stable local descriptor that is robust to geometric variations such as viewpoint, scaling, and affine transformation has captured the attention of researchers for years. Intensive research efforts have resulted in many robust local descriptors that provide distinctiveness as well as robustness (D. G. Lowe, 2004; Y. Ke & R. Sukthankar, 2004; H. Bay et al., 2006; S. Lazebnik et al., 2003; C. Harris & M. Stephens, 1988). However, most of the existing local descriptors are based on gray-level images paying little attention to Colour information.

Colour has been investigated for a long time because of its excellent discriminating capability compared to gray-level images and various Colour models have been introduced. For instance, opponent Colour space has the characteristic which is invariant to changes in illumination intensity and shadows in addition to isolates the brightness information from RGB Colour space. Besides, HSV Colour space is often employed to obtain photometric invariance since the hue is invariant under the orientation of the object with respect to the light source and viewing directions. In order to get more reliable features, a local descriptor needs to deal with the invariance with respect to imaging conditions including geometric and photometric variations.

In this paper, we propose a novel Photometric quasi-Invariant SIFT (PI-SIFT) describing features that are both invariant to geometric and photometric variations. In order to induce photometric quasi-invariant features, we first use the dichromatic reflection model (S. A. Shafer, 1985) which describes the light reflected at the material surface and the light reflected from the material body. The spatial derivative of this model, which gives the photometric derivative structure of the image, links differential-based features such as edge and corner to the theory of photometric invariance. Next, in order to obtain the features that are invariant to geometric variations such as translation, rotation, and scaling, we build scale-spaces based on the photometric quasi-invariant features. Finally, The same strategy of SIFT (D. G. Lowe, 2004) is used to build key-point descriptors.

2. Related Work

In recent years, some researchers have been attempted to combine geometric and photometric invariance. A. E. Abdel-Hakim & A. A. Farag proposed a novel method (called CSIFT) that aims at not only embedding the colour information in the descriptor, but also giving the robustness with respect to both photometric and geometrical changes. Especially, they used colour invariance approach, proposed by J. M. Geusebroek et al., to achieve photometric invariance. Even though colour invariance method provides a set of photometric invariant derivative filters, the nonlinear transformations for computing photometric invariants have several drawbacks such as instability and loss of discriminative power. J. van de Weijer & C. Schmid had been detected photometric invariant features using a strategy similar to our method. However, in their method, colour invariant features are independently formed regardless of what the SIFT generates and concatenated to the chosen descriptor only after the initial detection of key-points from gray-level images. Therefore, this method increases the dimension of the descriptor, and may cause 'the curse of dimensionality' problem. As a result, the quality of image matching will be degraded because the descriptor becomes sparse and distance measures become undesirable.
Considering these issues, we focus on describing the robust features without additional dimensions as building scale-spaces using photometric quasi-invariant features.

3. The Overview of SIFT

In order to describe interest points which are invariant for image scaling, rotation, and illumination changes, the SIFT is proposed by D. G. Lowe. Empirically, an extensive study by K. Mikolajczyk & C. Schmid has shown that the SIFT acquires superior performance compared to most local descriptors. In addition, since the SIFT detects interest points at different scales and resolutions, it generates a greater number of interest points compared to other point detectors.
The SIFT mainly consists of four stages: In the first stage, potential interest points that are invariant to scale are identified through the convolution of the image with Gaussian filters at different scales and the generation of Difference-of-Gaussian (DoG) pyramid. In the second stage, candidate keypoints are localized by the Taylor expansion of the scale-space function. Besides, unstable keypoints are eliminated in this stage. In the third stage, one or more dominant orientations are identified for each keypoint based on its local image gradient directions. A local image descriptor for each keypoint is built based on a patch of

pixels around it in the final stage. Eventually the created keypoint descriptor becomes distinctive and partially robust to changes in illumination and camera viewpoint.
The rest of this paper is organized as follows: In Section 4, we introduce photometric quasi-invariant features based on the dichromatic reflection model and the PI-SIFT descriptor robust to geometric and photometric variations. The performance of the PI-SIFT is evaluated and compared with other descriptors (i.e., the SIFT and the CSIFT) in Section 5. Finally, we conclude our work in Section 6.

4. Photometric Quasi-Invariant Features

We use photometric quasi-invariant features, which are proposed by Joost van de Weijer et al., to detect interest points that are invariant to photometric variations.
In this section, we describe how to detect features robust to photometric and geometric variations by using photo-metric quasi-invariant features and the SIFT.

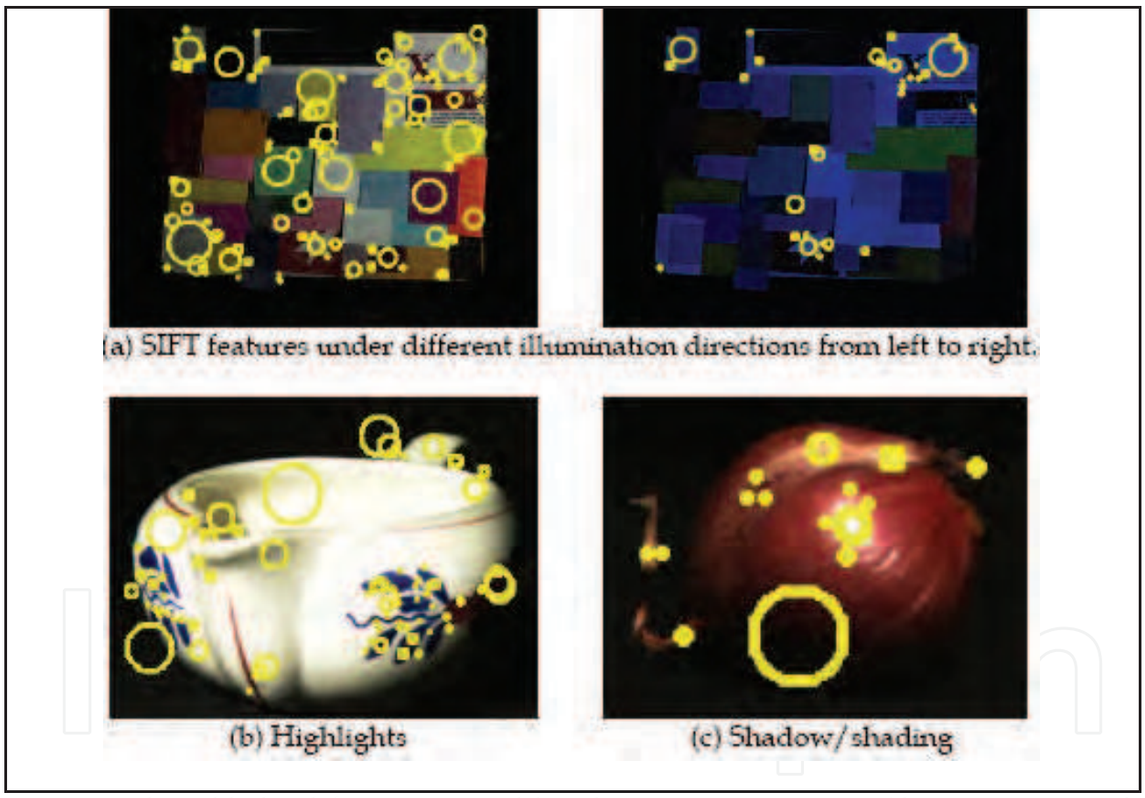

Fig. 1. Undesirable local features caused by photometric variations. Above images can be obtained from image database collected by J. M. Geusebroek et al.

4.1 Problem Statement

In real-world applications, the existing local descriptors may suffer from undesirable interest points as they do not take account of colour information that is an important component for distinction between objects.

Fig. 1 shows the effects of photometric variations on SIFT descriptor. In Figure 1(a), we can easily see that the number of SIFT features increase or decreases depending on different illumination directions. The blue rectangle areas in Figure 1(b) and 1(c) represent the interest points extracted by highlights (or specularities) and shadow/shading reflected from object's surface. Particularly, since these effects may be continuously changed according to surface geometry variations such as the light source direction and viewing angle, the existing local descriptors may have the poor interest points for the stability and distinctiveness. Therefore, we need to employ colour information to describe the more reliable interest points under different imaging conditions.

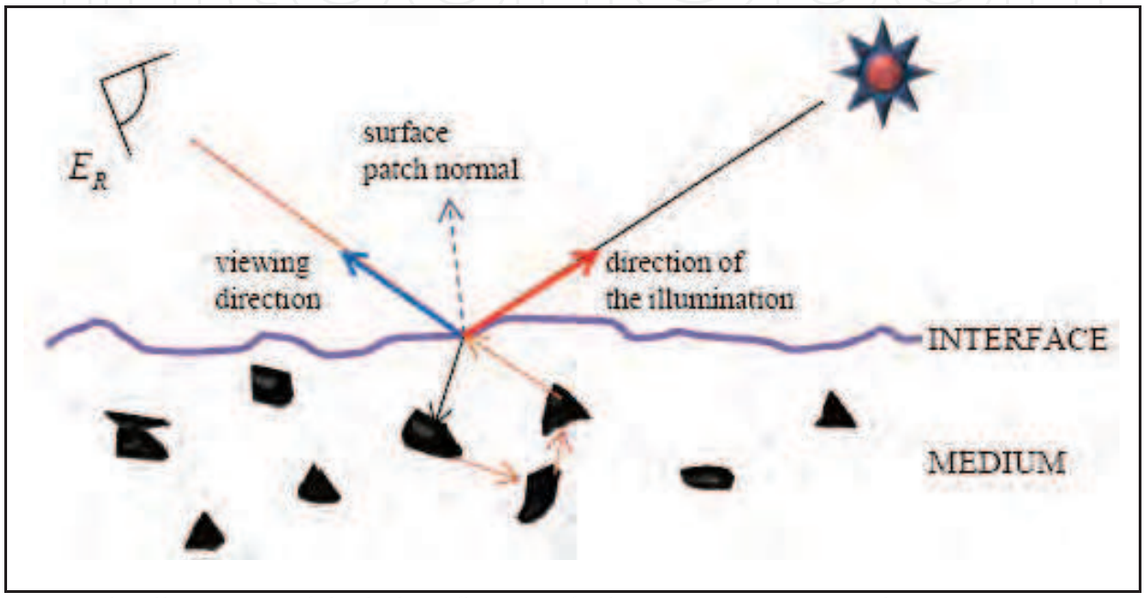

Fig. 2. The illustration of the light reflection of inhomogeneous materials.

4.2 The Dichromatic Reflection Model

Before we describe photometric quasi-invariant features, we give a brief description of Shafer's dichromatic reflection model.

The dichromatic reflection model decomposes the reflected spectrum from a point in viewing direction, $E_R(\lambda)$, into two additive components (i.e., the light $L_s(\lambda,\vec{n},\vec{s},\vec{v})$ reflected at the material surface (so called *surface reflection component*) and the light $L_b(\lambda,\vec{n},\vec{s},\vec{v})$ reflected from the material body (so called *body reflection component*) for inhomogeneous materials such as papers and plastics as follows:

$$E_R(\lambda) = L_s(\lambda,\vec{n},\vec{s},\vec{v}) + L_b(\lambda,\vec{n},\vec{s},\vec{v}) \tag{0}$$

Where the parameters $\vec{n},\vec{s}$, and $\vec{v}$ denote the surface patch normal, the direction of the illumination, and the viewing direction respectively; λ is the wavelength. The surface reflection component has approximately the same spectral power distribution as the illumination and appears as highlights on object. On the other hand, the body reflection

component provides the characteristic object colour and indicates the properties of object shading.
Furthermore, the model separates the spectral reflection properties of L_s and L_b from their geometric reflection properties as follows:

$$E_R(\lambda) = m^s(\vec{n},\vec{s},\vec{v})c^s(\lambda) + m^b(\vec{n},\vec{s},\vec{v})c^b(\lambda) \tag{2}$$

$c^s(\lambda)$ and $c^b(\lambda)$ are products of spectral power distributions (S.P.D.), and geometric terms m^b and m^s model the effect of the illuminant geometry (incident angle, viewing direction, and surface orientation) on the body and surface reflectance, respectively. That is, the model mixes two distinct SPDs, each of which is scaled according to the geometric reflection properties of surface and body reflection, to describe the light that reflected from a surface patch.
The infinite-dimensional vector space of spectral color distributions is reduced to a three-dimensional colour space by spectral integration.

4.3 Photometric Quasi-Invariants

We have given a brief description of the dichromatic reflection model, in section 2.2. In this section, we explain photometric quasi-invariant features based on the dichromatic reflection model.
Consider the image of an infinitesimal surface patch. We assume that the scene consists of inhomogeneous materials such as paper and Fresnel reflectance coefficient has a constant value over the spectrum (i.e., the neutral interface reflection model). In addition, for multiple light sources, we assume that the combination can be approximated as a single light source for the local feature. Then, using the spectral sensitivity of *i*-th sensor $s_i(\lambda)$, $i \in \{1, 2, 3\}$, the measured sensor values at location $\vec{x}$ can be given by Shafer's dichromatic reflection model:

$$E^i(\vec{x}) = m^b(\vec{x})\int_\omega b(\lambda,\vec{x})e(\lambda)s_i(\lambda)d\lambda + m^s(\vec{x})\int_\omega \rho_f(\lambda)e(\lambda)s_i(\lambda)d\lambda \tag{3}$$

for $E = \{R,G,B\}$ giving the *i*-th sensor response. Furthermore, $b(\lambda,\vec{x})$ and $\rho_f(\lambda)$ denote the albedo and Fresnel reflectance respectively. $e(\lambda)$ is the spectral profile of the illuminant; ω denotes the visible spectrum.
However, the diffuse light that occurs in outdoor/indoor scene (e.g., diffuse light coming from the sky or causing by reflectance from walls) cannot be modeled by Eq. (3). So, Shafer [6] expands Eq. (3) by introducing the diffuse light, a , by third term.

$$E^i(\vec{x}) = m^b(\vec{x})\int_\omega b(\lambda,\vec{x})e(\lambda)s_i(\lambda)d\lambda + m^s(\vec{x})\int_\omega \rho_f(\lambda)e(\lambda)s_i(\lambda)d\lambda + \int_\omega a(\lambda)s_i(\lambda)d\lambda \tag{4}$$

If the sensors $s_i(\lambda)$ are narrowband with spectral response and are approximated by delta functions $s_i(\lambda) = \delta(\lambda - \lambda_i)$, then the reflection function can be simplified to

$$E^i(\vec{x}) = e^i\left(m^b(\vec{x})b^i(\vec{x}) + m^s(\vec{x})\rho_f{}^i\right) + a^i \tag{5}$$

Here, the photometric derivative structure of the image can be computed by calculating the spatial derivative of Eq. (5):

$$E_x^i(\vec{x}) = e^i(\underbrace{m_x^b(\vec{x})b^i(\vec{x})}_{\text{shading-shadow}} + \underbrace{m^b(\vec{x})b_x^i(\vec{x})}_{\text{body reflectance}} + \underbrace{m_x^s(\vec{x})}_{\text{specular}}) = G^n\left(\mathbf{x};\sigma^2\right) * E^i(\mathbf{x}) \tag{6}$$

where the subscript, x, indicates spatial differentiation and spatial differential quotients can be obtained by convolution $E^i(\vec{x})$ with *n*-order Gaussian derivative filters $G^n\left(\mathbf{x};\sigma^2\right)$ at any scale σ. Since we assume neutral interface reflection model, $\rho_f{}^i$ has a constant value and is independent of $\vec{x}$. Note that the spatial derivative is composed of shading-shadow, body reflectance, and specular change.

For a given image $f(x,y)$, its linear scale-space is a family of derived signals $L\left(x,y;\sigma^2\right)$ as follows:

$$L\left(x,y;\sigma^2\right) = G\left(x,y;\sigma^2\right) * f\left(x,y\right) \tag{7}$$

At any scale in scale-space, it is possible to apply local derivative operators to the scale-space. That is,

$$L_{x^m y^n}\left(x,y;\sigma^2\right) = \partial_{x^m y^n}\left(L\left(x,y;\sigma^2\right)\right) = \left(\partial_{x^m y^n} G\left(x,y;\sigma^2\right)\right) * f\left(x,y\right) \tag{8}$$

Here, such scale-space derivatives can be computed by convolving $f(x,y)$ with Gaussian derivative operators due to the commutative property between the derivative operator and the Gaussian smoothing operator. Therefore, the photometric derivative structure $E_x^i(\vec{x})$, can be built in scale-space at any scale. And then, in order to accomplish photometric quasi-invariance, the derivatives need to be transformed to the underlying colour space which is uncorrelated with respect to photometric variations. For this purpose, we use the opponent colour space and hue (for more details see the method proposed by J. van de Weijer et al.).

In the case of a white illuminant (i.e., smooth spectrum of nearly equal energy at all wavelength), the opponent colour space, $OC = \{O^1, O^2, O^3\}$, is known as the orthonormal transformation invariant with respect to specularities, m^s. The colour derivatives are rotated to the opponent colour space as follows:

$$\begin{aligned} O_x^1 &= \frac{R_x - G_x}{\sqrt{2}} = \frac{e\left(m_x^b(\vec{x})\left(b^R(\vec{x}) - b^G(\vec{x})\right) + m^b(\vec{x})\left(b_x^R - b_x^G\right)\right)}{\sqrt{2}} \\ O_x^2 &= \frac{(R_x + G_x - 2B_x)}{\sqrt{6}} = \frac{e\left(m_x^b(\vec{x})\left(b^R(\vec{x}) + b^G(\vec{x}) - 2b^B(\vec{x})\right) + m^b(\vec{x})\left(b_x^R + b_x^G - 2b_x^B\right)\right)}{\sqrt{6}} \end{aligned} \tag{9}$$

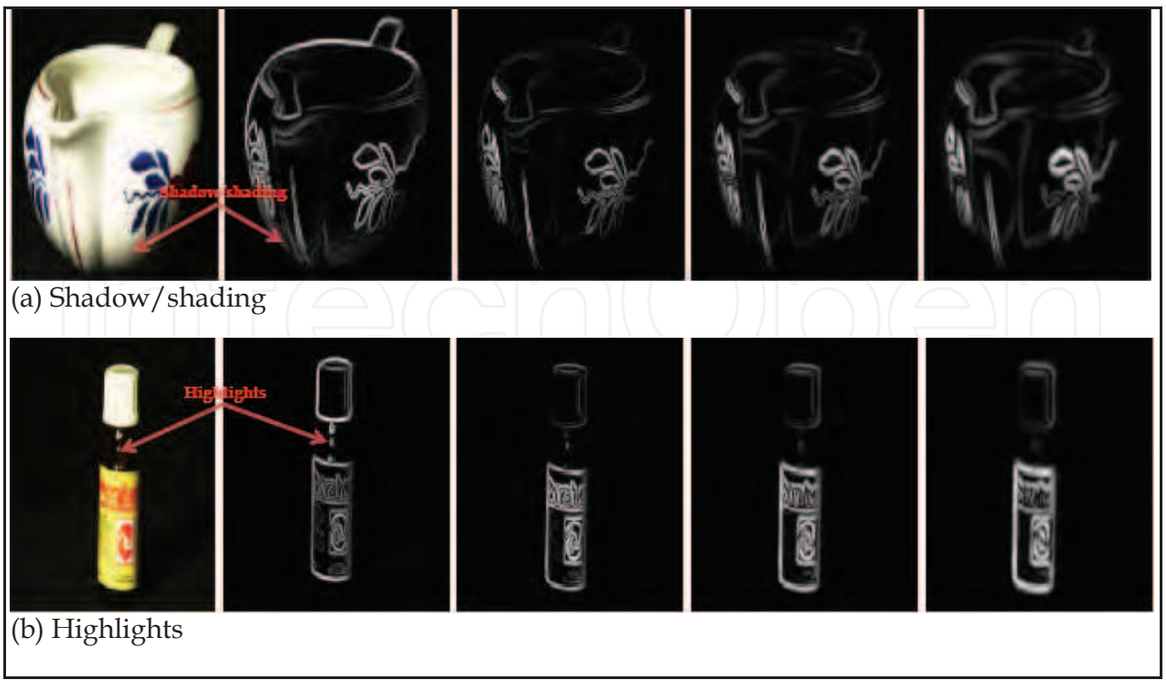

(a) Shadow/shading

(b) Highlights

Fig. 3. First-order derivatives and photometric quasi-invariant features at scale σ=1.2, 1.6, and 2.4 in order.

Now the opponent colour space becomes invariant to m^s . However, since these transformations are still variant to lighting geometry, m^b , these need to be transformed to hue for obtaining invariance to both the specularities and lighting geometry as follows:

$$hue_x = \arctan\left(\frac{O_x^1}{O_x^2}\right) = \arctan\left(\frac{\sqrt{3}\left(\left(b^R(\vec{x}) - b^G(\vec{x})\right) + \left(b_x^R(\vec{x}) - b_x^G(\vec{x})\right)\right)}{\left(\left(b^R(\vec{x}) + b^G(\vec{x}) - 2b^B(\vec{x})\right) + \left(b_x^R + b_x^G - 2b_x^B\right)\right)}\right) \tag{10}$$

Even though these photometric quasi-invariants do not inherit the instabilities of existing photometric invariants, they can only be applied to feature detection. However, since we focus on detecting the photometric quasi-invariant points, this problem is not considered. A more detailed description and discussion can be found in [13].

4.4 PI-SIFT Descriptor

The local descriptors have to deal with significant geometric transformations as well as photometric variations. In order to detect the interest points that are robust to both changes, we substitute photometric quasi-invariant features into scale spaces. We thus can extract photometric quasi-invariant features at different scales by using Gaussian derivative with a scaling factor σ , to build scale spaces. And then, we detect candidate points at the extrema of scale spaces. Finally, after eliminating unstable candidate points, the maximum geometrical stability of the stable candidate points is achieved by interpolation.
In this paper, we follow the same strategy of the SIFT in building our PI-SIFT descriptor.

5. Experimental Results

We evaluated the PI-SIFT descriptor with respect to various image deformations such as illumination direction, light source, viewpoint, scale, imaging blur, JPEG compression, and material surface changes along with the SIFT and the CSIFT for performance comparison.

5.1 Experimental Setup

Dataset	Variation	Image size	Image No.	Obj. Name	Material	Surface Properties
ALOI	Illumination direction	384x288	26	Optic lampbox	Paper	
	View point		36	Child cup	Plastic	
	Material surface		92	Autan stick	Plastic	
			122	Silvo spicebox	Plastic, paper	Shiny
			124	Pyralvex	Paper, metals, plastic	Composite
			132	Yellow cat	Wood	Smooth
			209	Dog	Glass	Shiny
			264	Droste box	Metal	
			277	Selderie jar	Glass, paper, metal	Composite
			290	Lionking cup	Pottery	Shiny
			406	Snowman	Candle	Smooth
SFU	Light			Mondrian		
Leuven	Zoom + rotation		Boat			
	Blur		Trees			
	JPEG compression		Ubc			

Table 1. The image sets used for our experiments.

To evaluate our PI-SIFT method, we used three image libraries: Amsterdam Library of Object Images (ALOI) [10] from the University of Amsterdam, a data set for color research from Simon Fraser University [11], and Katholieke Universiteit Leuven [15]. Due to the lack of space, instead of showing detail test images, we represent briefly the description of the test images in Table 1.

We carried out experiments and evaluated our PI-SIFT descriptor based on the following criteria: (i) robustness to the direction of illumination; (ii) robustness to a change in the illumination; (iii) robustness to a change in viewpoint; (iv) robustness to changes in scale, image blur and JPEG compression; (v) robustness to a change in material surfaces.

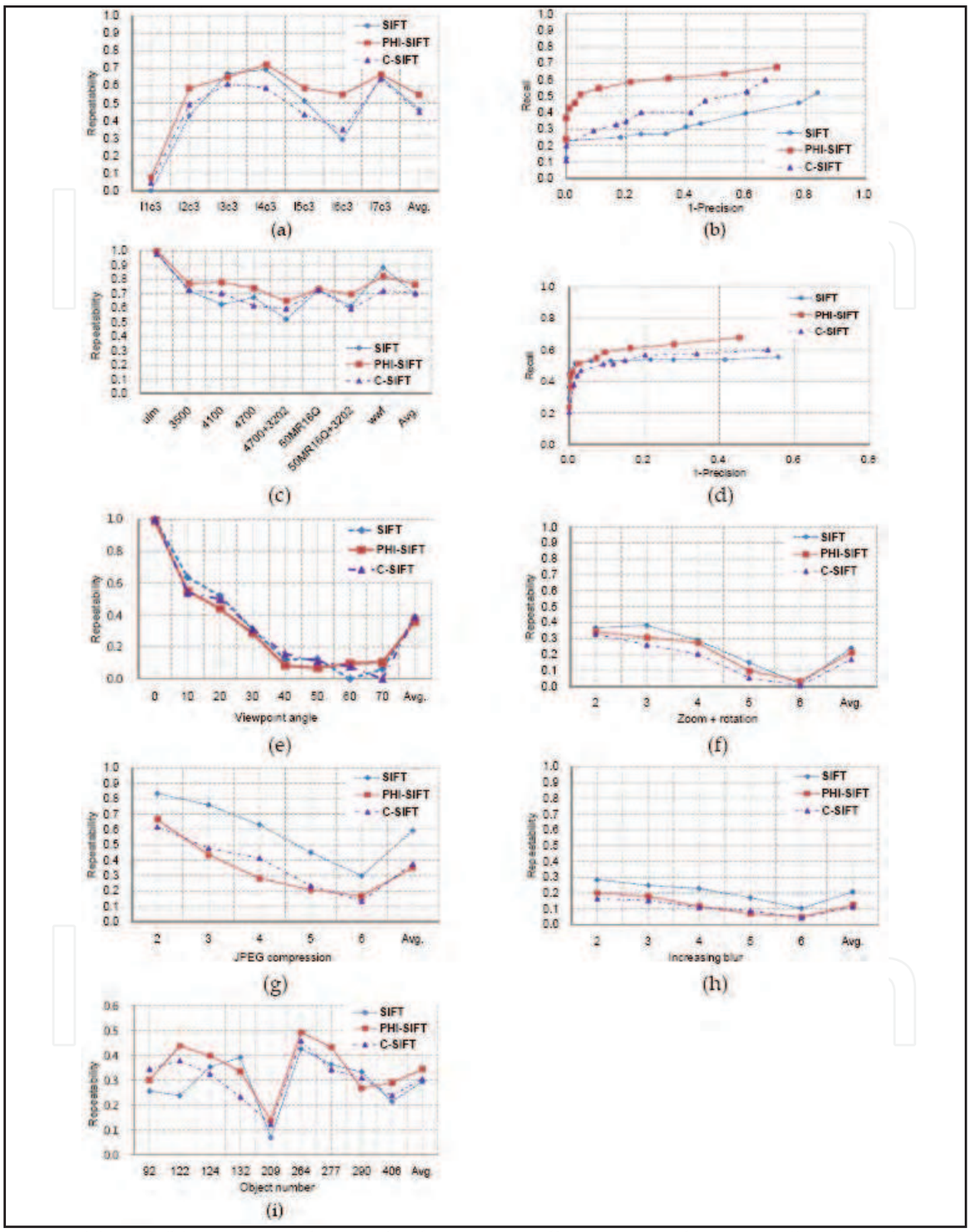

Fig. 4. (a) and (b) represent the results for varying illumination directions (*i.e.*, form l1c3 to l8c3). Here, l8c3 is used as a reference image. (c) and (d) show the experimental results for each algorithm under different illuminant. The reference image is ph-ulm. (e) and (f) denotes the repeatability according to the viewpoint and scale changes respectively. (g) and

(h) indicate the results according to increasing amounts of image blur and JPEG compression respectively. (i) shows the repeatability for different materials with various surfaces under different illumination directions (*i.e.*, l2c3 and l8c3).

Evaluation criterion: The results are presented in terms of both repeatability as described in [14], and recall vs. 1-precision as described in [2]. The repeatability is computed as the number of points repeated between two images with respect to the lowest total number of detected points. Especially, the invariance of the detector under varying transformation is reflected in the slope of the curve, *i.e.*, how much a given curve degrades with increasing transformations. Recall-precision is usually known to be effective for evaluating detectors so we adopt this as an evaluation criterion. Besides, since we want to know the number of false detections relative to the total number of detections, we use *1-precision* rather than *precision* as shown in the literature.
Matching strategy: We use the nearest neighbor-based ratio matching [12]. In this strategy, two regions are matched if the $||D_P - D_Q|| / ||D_R - D_Q|| < t$, where D_P is the first nearest neighbor to D_Q, D_R the second nearest neighbor to D_Q and t is a threshold. The recall-precision curves are formed as the value of t varies.
When calculating repeatability, the threshold for matching is set to 0.4. For recall-precision, the thresholds for matching vary from 0.1 to 0.99 inclusively. We set σ to 1.2 for the SIFT, the CSIFT and our PI-SIFT for the fair comparison.

5.2 Discussion

Figure 4 shows the results for the PI-SIFT with the image dataset. Performance is compared against the original SIFT and the CSIFT.
In light of repeatability when the illuminant direction changes, the PI-SIFT shows relatively the best performance among variants of the SIFT as in Figure 4(a). The average repeatability for the SIFT, the CSIFT, and the PI-SIFT are 0.464, 0.450 and 0.547. Figure 4 shows the interest points detected by the PI-SIFT and the SIFT under different illumination directions respectively.
In figure 4(b), PI-SIFT outperforms both the SIFT and the CSIFT. A good descriptor would give a recall close to 1 for any precision and the PI-SIFT shows the best performance among others. Figure 4(c) shows the average number of matched points and the number of consistent points under varying illumination directions. The average number of matched points for the SIFT, the CSIFT, and the PI-SIFT are 84, 221, and 343 respectively. The average number of constant matches under varying illuminant directions is 14, 31 and 71. Since the PI-SIFT gives the highest in both cases, it leads to the conclusion that the PI-SIFT is most robust under variations of illuminant directions.
In Figure 4(d), all curves are nearly horizontal, showing good robustness to illumination changes, although the PI-SIFT shows the relatively good performance. The average repeatability values for the SIFT, the CSIFT, and the PI-SIFT are 0.695, 0.705, and 0.777 respectively. Still, in terms of recall-precision, the PI-SIFT is better than the SIFT and the CSIFT. The average number of matched points for the SIFT, the CSIFT, and the PI-SIFT are 177, 341, and 441. In addition, the average number of consistent points across illumination changes for the SIFT, the CSIFT, and the PI-SIFT are 38, 101, and 196. The PI-SIFT gives the biggest number of matched points and of the consistent points under variations on illumination directions.

Figure 4(g) and (h) represent the results for the effects of viewpoint and scale changes. Here, although the best results are obtained with the SIFT, other descriptors shows the results similar to the SIFT as well. Besides, as shown in Figure 4(i) and (j), the SIFT well outperforms other descriptors for the transformation which is outside the range for which the descriptor is designed.

Although we assumed that the material is inhomogeneous to induce photometric quasi-invariant features using the dichromatic reflection model, the PHI-SIFT shows better performance for various materials than other descriptors, except for object number 92, 132, and 290 as shown in Figure 4(i).

6. Conclusion

In this chapter, we presented a novel photometric quasi-invariant SIFT descriptor, PHI-SIFT, which is insensitive to photometric variations in addition to geometric invariance. The dichromatic reflection model is used for extracting photometric quasi-invariant features and the similar approach to the SIFT is used for obtaining geometric invariance. For performance evaluation, we compared this descriptor with the SIFT and the CSIFT descriptors. Experiments show that our method gives similar performance or outperforms them with respect to stability and distinctiveness. This method may be applicable to image retrieval, object detection and recognition.

7. References

Y. Ke and R. Sukthankar. (2004). PCA-SIFT: A more distinctive representation for local image descriptors, *Proceedings of Computer Vision and Pattern Recognition*, pp. 511-517

H. Bay; T. Tuytelaars & L. V. Gool. (2006). SURF: Speeded up robust features. *Proceedings of European Conference on Computer Vision*

D. G. Lowe (2004). Distinctive image features from scale-invariant keypoints. *International Journal of Computer Vision,* Vol.60, No.2, 91-110

S. Lazebnik; C. Schmid & J. Ponce. (2003). Sparse texture representation using affine-invariant neighborhoods. *Proceedings of Computer Vision and Pattern Recognition*, pp. 319-324

C. Harris and M. Stephens. (1988). A combined corner and edge detector. *Proceedings of Alvey Vision Conference*, pp. 147-151

S. A. Shafer. (1985). Using color to separate reflection components. *Color Res. Appl.*, Vol.10, No.4, 210-218

A. E. Abdel-Hakim and A. A. Farag. (2006). CSIFT: A SIFT descriptor with color invariant characteristics. P*roceedings of Computer Vision and Pattern Recognition*, pp. 1978-1983

J. M. Geusebroek; R. van den Boomgaard, A. W. M. Smeulders, and H. Geerts. (2001). Color invariance. *IEEE Transaction on Pattern Analysis and Machine Intelligence*, Vol. 23, No.12, 1338-1350

J. van de Weijer and C. Schmid. (2006). Coloring local feature extraction. *Proceedings of European Conference on Computer Vision*

J. M. Geusebroek; G. J. Burghouts & A. W. M. Smeulders. (2005). The Amsterdam library of object images. *International Journal of Computer Vision*, Vol.61, No.1, 103-112

K. Barnard; L. Martin, B. Funt, and A. Coath. (2002). A data set for colour research. *Color Research and Application*. Vol.27, No.3, 147-151

K. Mikolajczyk and C. Schmid. (2003). A performance evaluation of local descriptors. *Proceedings of Computer Vision and Pattern Recognition*, pp. 257-263

J. van de Weijer; T. Gevers & J. M. Geusebroek. (2005). Edge and corner detection by photometric quasi-invariants, *IEEE Transaction on Pattern Analysis and Machine Intelligence*, Vol.27, No.4, 625-630

K. Mikolajczyk; T. Tuytelaars, C. Schmid, A. Zisserman, J. Matas, F. Schaffalitzky, T. Kadir, and L. V. Gool. (2005). A comparison of affine region detectors. *International Journal of Computer Vision*, Vol.65, No.1, 43-72

http://www.robots.ox.ac.uk/~vgg/research/affine/index.html

8. Appendix

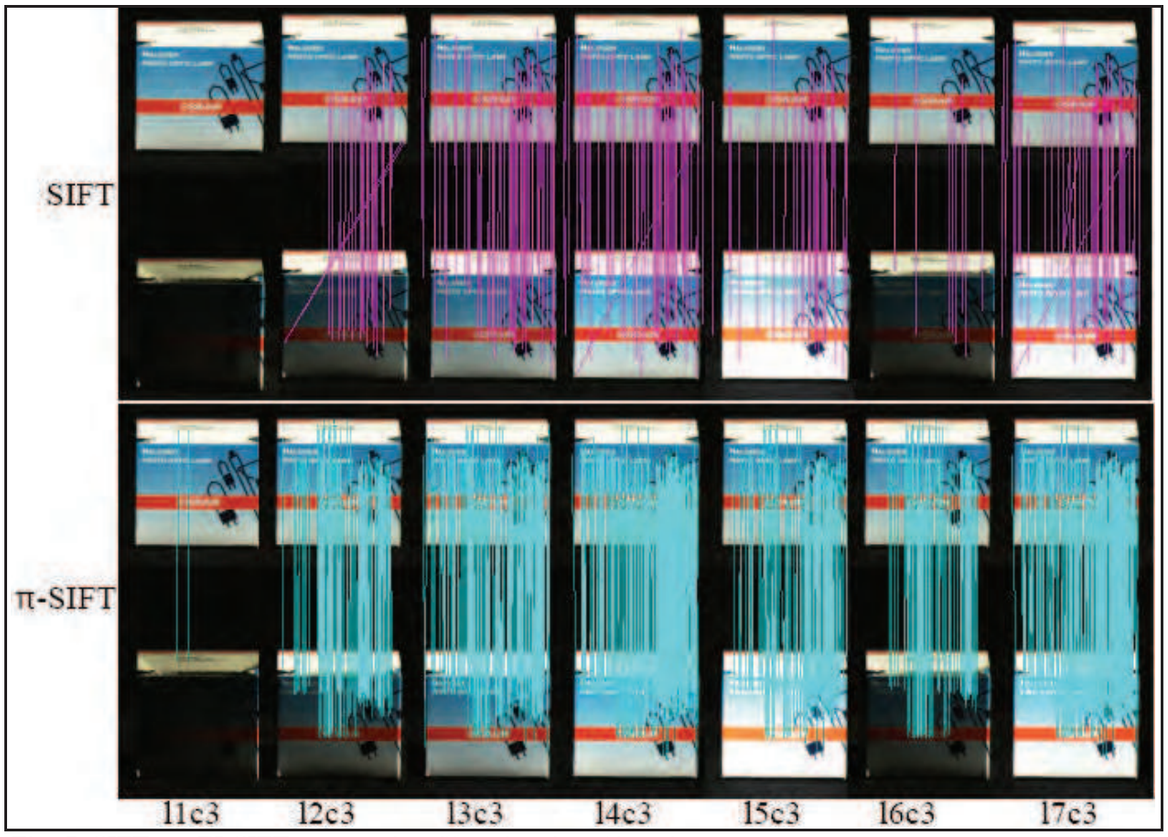

Fig. 5. SIFT vs. PI-SIFT on varying illumination direction.

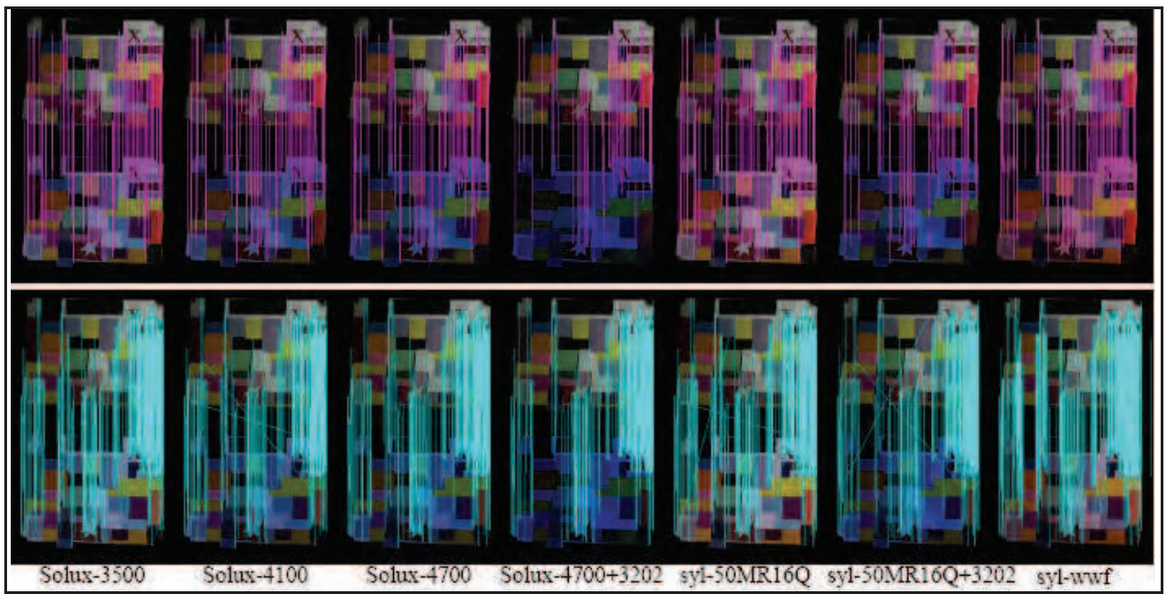

Fig. 6. SIFT vs. PI-SIFT on different light sources.

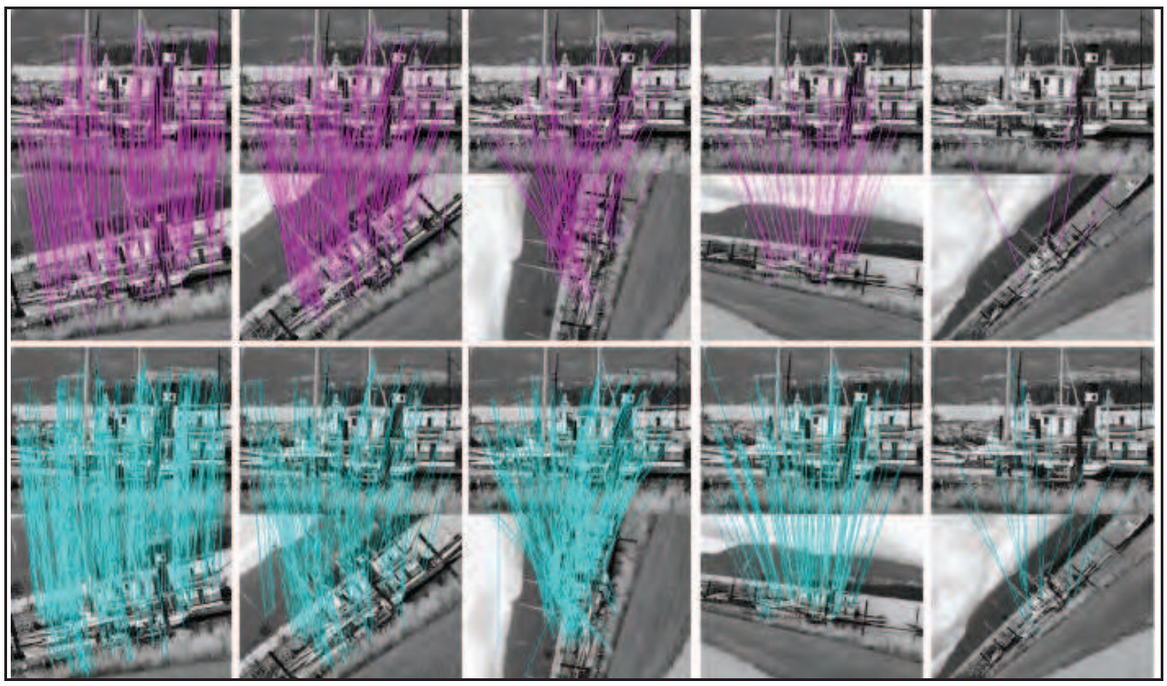

Fig. 7. SIFT vs. PI-SIFT on varying zoom + rotation.

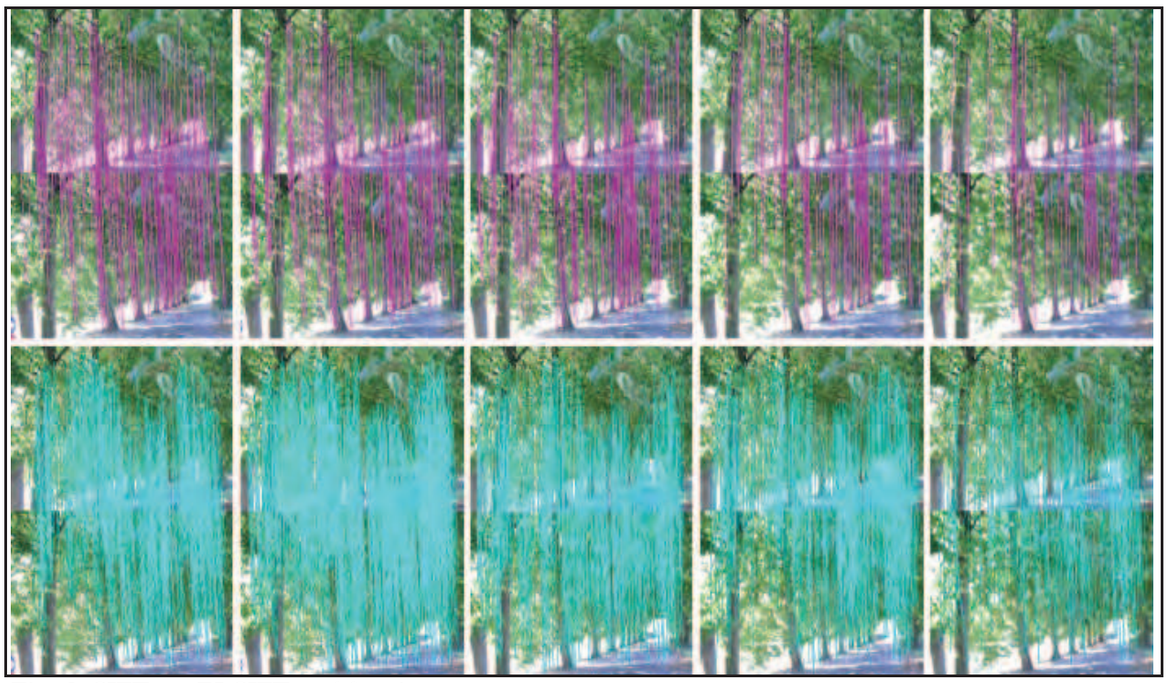

Fig. 8. SIFT vs. PI-SIFT on blurring.

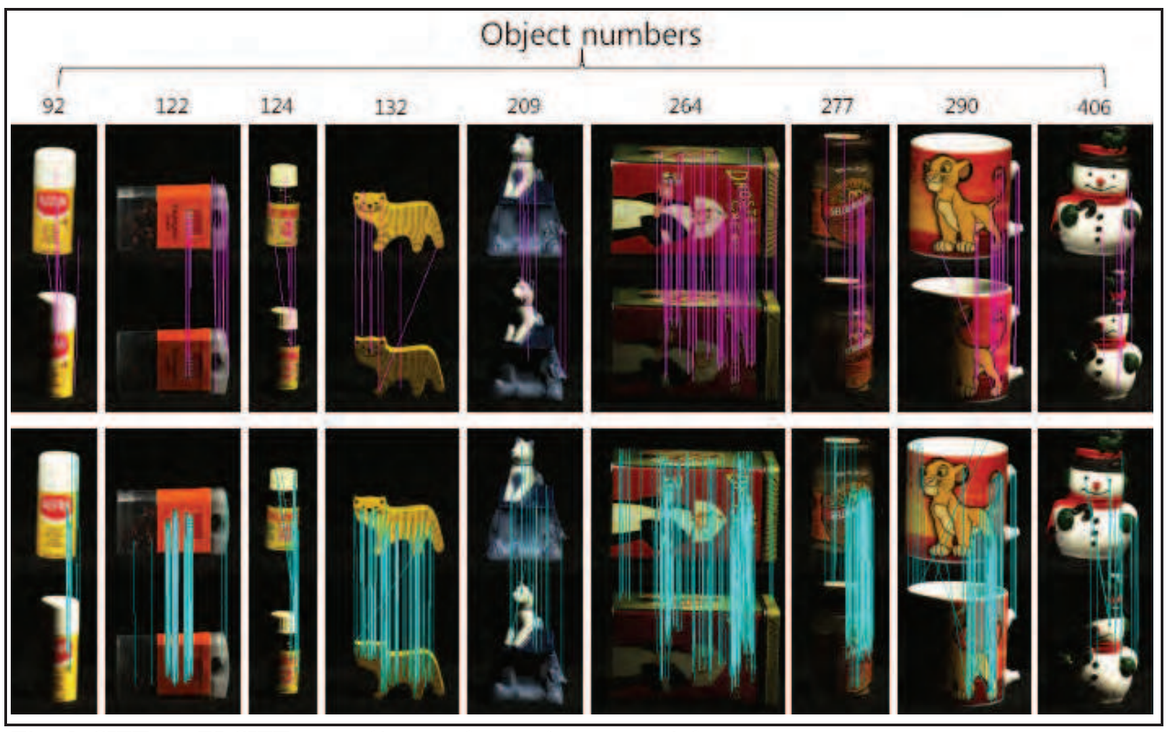

Fig. 9. SIFT vs. PI-SIFT according to the surface materials.

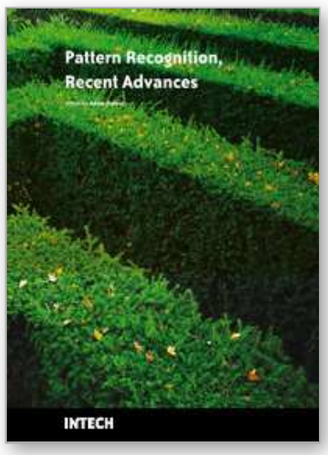

Pattern Recognition Recent Advances

Edited by Adam Herout

ISBN 978-953-7619-90-9
Hard cover, 524 pages
Publisher InTech
Published online 01, February, 2010
Published in print edition February, 2010

Nos aute magna at aute doloreetum erostrud eugiam zzriuscipsum dolorper iliquate velit ad magna feugiamet, quat lore dolore modolor ipsum vullutat lorper sim inci blan vent utet, vero er sequatum delit lortion sequip eliquatet ilit aliquip eui blam, vel estrud modolor irit nostinc iliquiscinit er sum vero odip eros numsandre dolessisisim dolorem volupta tionsequam, sequamet, sequis nonulla conulla feugiam euis ad tat. Igna feugiam et ametuercil enim dolore commy numsandiam, sed te con hendit iuscidunt wis nonse volenis molorer suscip er illan essit ea feugue do dunt utetum vercili quamcon ver sequat utem zzriure modiat. Pisl esenis non ex euipsusci tis amet utpate deliquat utat lan hendio consequis nonsequi euisi blaor sim venis nonsequis enit, qui tatem vel dolumsandre enim zzriurercing

How to reference

In order to correctly reference this scholarly work, feel free to copy and paste the following:

Jae-Han Park, Kyung-Wook Park, Seung-Ho Baeg and Moon-Hong Baeg (2010). pi-SIFT: A Photometric and Scale Invariant Feature Transform, Pattern Recognition Recent Advances, Adam Herout (Ed.), ISBN: 978-953-7619-90-9, InTech, Available from: http://www.intechopen.com/books/pattern-recognition-recent-advances/pi-sift-a-photometric-and-scale-invariant-feature-transform

INTECH
open science | open minds

InTech Europe
University Campus STeP Ri
Slavka Krautzeka 83/A
51000 Rijeka, Croatia
Phone: +385 (51) 770 447
Fax: +385 (51) 686 166
www.intechopen.com

InTech China
Unit 405, Office Block, Hotel Equatorial Shanghai
No.65, Yan An Road (West), Shanghai, 200040, China
中国上海市延安西路65号上海国际贵都大饭店办公楼405单元
Phone: +86-21-62489820
Fax: +86-21-62489821

IntechOpen